

Forward Physics with the CMS Experiment at the Large Hadron Collider*

Dmytro Volyanskyy^{†‡}
Deutsche Elektronen-Synchrotron DESY
Notkestrasse 85, 22607 Hamburg, Germany

The forward physics program of the CMS experiment at the LHC spans a broad range of diverse physics topics including studies of low- x QCD and diffractive scattering, multi-parton interactions and underlying event structure, γ -mediated processes and luminosity determination, Monte Carlo tuning and even MSSM Higgs discovery in central exclusive production. In this article, the forward detector instrumentation around the CMS interaction point is described and the prospects for diffractive and forward physics using the CMS forward detectors are summarized. In addition, first observation of forward jets as well as early measurements of the forward energy flow in the pseudorapidity range $3.15 < |\eta| < 4.9$ at $\sqrt{s} = 0.9$ TeV, 2.36 TeV and 7 TeV are presented.

PACS numbers:

Keywords: forward physics, diffraction, energy flow

I. THE CMS EXPERIMENT AT THE LHC

The Compact Muon Solenoid (CMS) [1] is one of two general-purpose particle physics detectors built at the Large Hadron Collider (LHC) at CERN. The detector has been designed to study various aspects of proton-proton (pp) collisions at $\sqrt{s} = 14$ TeV and heavy-ion (Pb-Pb) collisions at $\sqrt{s} = 5.5$ TeV, that will be provided by the LHC at a design luminosity of 10^{34} $\text{cm}^{-2}\text{s}^{-1}$ and of 10^{27} $\text{cm}^{-2}\text{s}^{-1}$, correspondingly. To enhance the physics reach of the experiment the CMS subcomponents must provide high-precision measurements of the momentum and the energy of collision-products. The CMS detector comprises the tracking system covering the pseudorapidity range $-2.5 < \eta < 2.5$ and the calorimetry system covering the pseudorapidity range $-5 < \eta < 5$. In addition to that, CMS includes several very forward calorimeters, whose design and physics potential will be described later in this article. It should be emphasized that the CMS detector is one of the largest scientific instruments ever built. It comprises about 76.5 millions of readout channels in total. The detector has been designed, constructed and currently operated by the collaboration consisting of more than 3500 scientists from 38 countries.

First collision data taking at CMS took place in November 2009. Since then and by the end of May 2010, CMS has collected around 10 nb^{-1} of collision data. It should be noted that the quality of collected data is rather good: more than 99% of CMS readout channels are operational and the CMS data taking efficiency is above 90%. Several tens of pb^{-1} of the pp collision data are expected to be collected by the end of 2010.

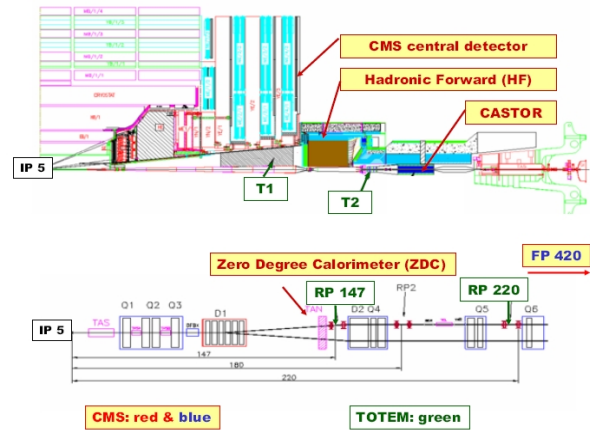


Figure 1: Layout of the forward detectors around the CMS interaction point.

II. FORWARD DETECTORS AROUND THE CMS INTERACTION POINT

The maximum possible rapidity at the LHC in pp collisions at $\sqrt{s} = 14$ TeV is $y_{max} = \ln(\sqrt{s}/m_{\pi}) \approx 11.5$ and one of the great features of the CMS experiment is that it includes several subdetectors covering the kinematic region at very small polar angles and so, large values of rapidity. A schematic view of CMS forward detectors is shown in Figure 1. As can be seen, the CMS forward instrumentation consists of the Hadronic Forward calorimeter (HF), the CASTOR and ZDC calorimeters. All of them are sampling calorimeters. That is, they are made of repeating layers of a dense absorber and tiles of scintillator. A separate experiment TOTEM as well as proton detectors FP420 are additional forward detectors around the CMS interaction point (IP5). They further extend the forward reach available around IP5.

[†]on behalf of the CMS collaboration

*Presented at Forward Physics at LHC Workshop (May 27-29, 2010), Elba Island, Italy

[‡]Electronic address: Dmytro.Volyanskyy@cern.ch

A. HF

The CMS HF detector [2] includes two calorimeters HF+ and HF-, which are located at a distance of 11.2 m on the both sides from the IP5 covering the pseudorapidity range $3 < |\eta| < 5$. The detector is designed to carry out the measurements of the forward energy flow and forward jets. The HF is a Cerenkov sampling calorimeter which uses radiation hard quartz fibers as the active material and steel plates as the absorber. The signal in the HF is produced when charged shower particles pass through the quartz fibers with the energy above the Cerenkov threshold (190 keV for electrons). The generated Cerenkov light is then collected by air-code light guides, which are connected to photo-multiplier tubes PMTs. The detector fibers run parallel to the beamline and are bundled to form 0.175×1.175 ($\Delta\eta \times \Delta\phi$) towers. Half of the fibers run over the full depth of the absorber, whereas the other half starts at a depth of 22 cm from the front of the detector. These two sets of fibers are read out separately. Such a structure allows to distinguish showers generated by electrons and photons, which deposit a large fraction of their energy in the first 22 cm, from those generated by hadrons, which produce signals in both calorimeter segments. The detector is embedded into a cylindrical steel structure with the outer radius of 131 cm and the inner radius of 12.5 cm to accommodate the beam pipe. It is azimuthally subdivided into 20^0 modular wedges, each of which consists of two azimuthal sectors of 10^0 . The detector extends over 10 interaction lengths and includes 1200 towers in total.

B. CASTOR

The CASTOR (Centauro And STrange Object Research) detector [3] is a quartz-tungsten Cerenkov sampling calorimeter, which is located at a distance of 14.4 m from the IP5 and covering the pseudorapidity range $-6.6 < \eta < -5.2$. The tungsten metal has been chosen as the absorber medium in CASTOR, since it provides the smallest possible shower size. In this detector, the radiation hard quartz plates used as the active medium are tilted at 45^0 to efficiently capture the Cerenkov light produced by relativistic particles passing the detector. As in the case of the HF, the produced Cerenkov light is collected by air-code light guides that are connected to PMTs, which produce signals proportional to the amount of light collected. The CASTOR detector is a compact calorimeter with the physical size of about $65 \text{ cm} \times 36 \text{ cm} \times 150 \text{ cm}$ and having no segmentation in η . It is embedded into a skeleton, which is made of stainless steel. The detector consists of 14 longitudinal modules, each of which comprises 16 azimuthal sectors that are mechanically organized in two half calorimeters. First 2 longitudinal modules form the electromagnetic section, while the other 12 modules form the hadronic section. In the electromagnetic section, the

thicknesses of the tungsten and quartz plates are 5.0 and 2.0 mm respectively, whereas in the hadronic section the corresponding thicknesses are 10.0 and 4.0 mm. With this design, the diameter of the showers of electrons and positrons produced by hadrons is about one cm, which is an order of magnitude smaller than in other types of calorimeters. The detector has a total depth of 10.3 interaction lengths and includes 224 readout channels.

C. ZDC

The CMS ZDC (Zero Degree Calorimeter) detector [4] consists of two calorimeters that are located inside the TAN absorbers at the ends of the straight section of the LHC beam pipe at a distance of 140 m on both sides from the IP5. These are Cerenkov sampling calorimeters with quartz fibers as the active material and tungsten plates as the absorber material. The ZDC detector is designed to measure neutrons and very forward photons providing detection coverage in the pseudorapidity region $|\eta| > 8.4$. Each ZDC is made up of separate electromagnetic and hadronic sections. The electromagnetic section consists of 33 layers of 2 mm thick tungsten plates and 33 layers of 0.7 mm thick quartz fibers. The hadronic section is made of 24 layers of 15.5 mm thick tungsten plates and 24 layers of 0.7 mm thick quartz fibers. The electromagnetic section is segmented into 5 horizontal individual readout towers, whereas the hadronic section is longitudinally segmented into 4 readout segments. The tungsten plates are oriented vertically in the electromagnetic section whereas they are tilted by 45^0 in the hadronic section. The detector is read out via aircore light guides and PMTs. It has a total depth of 6.5 interaction length.

D. TOTEM and FP420

TOTEM [5] is an independent experiment at the CMS interaction point whose main objectives are the precise measurement of the total pp cross-section and a study of elastic and diffractive scattering at the LHC. To achieve optimum forward coverage for charged particles, TOTEM comprises two tracking telescopes, T1 and T2, that are installed on both sides from the IP5 in the pseudorapidity region $3.1 < |\eta| < 6.5$, and Roman Pot stations that are located at distances of $\pm 147 \text{ m}$ and $\pm 220 \text{ m}$ from the IP5. The T1 telescope is located in front of HF and consists of 5 planes of cathode strip chambers, while the T2 telescope is located in front of CASTOR and comprises 10 planes of gas electron multipliers. For efficient reconstruction of very forward protons, silicon strip detectors are housed in the Roman Pot stations.

FP420 [6] is a proposed detector system, which is supposed to provide proton detection at a distance of $\pm 420 \text{ m}$ from the IP5. The FP420 detector comprises a silicon tracking system that can be moved transversely and measure the spatial position of protons, which have been bent

out by the LHC magnets due to the loss of a small fraction of their initial momentum. The potential physics topics that can be studied with this detector system include Higgs central exclusive production as well as a rich QCD and electroweak program.

III. PHYSICS PROGRAM

Extending the physics reach of CMS, the program for forward physics includes studies of low- x QCD and diffractive scattering, multi-parton interactions and underlying event structure, γ -mediated processes and luminosity determination. It is also supposed to contribute to the discovery physics via searches of MSSM Higgs in central exclusive production.

A. Low- x QCD

A study of QCD processes at a very low parton momentum fraction $x = p_{parton}/p_{hadron}$ is a key to understand the structure of the proton, whose gluon density is poorly known at very low values of x . Low- x QCD dynamics can be studied in pp collisions if the parton momentum fraction of one of the colliding protons x_1 is significantly larger than the parton momentum fraction of the other colliding proton x_2 ($x_1 \gg x_2$). The result of such a collision is a creation of either jets, prompt- γ or Drell-Yan electron pairs at very low polar angles in the very forward region of the detector. Low- x QCD studies at CMS will be a continuation of studies of deep inelastic scattering in electron-proton collisions at HERA, where low- x QCD dynamics has been explored down to values of 10^{-5} . Measurements at HERA have shown that the gluon density in the proton rises rapidly with decreasing values of x . As long as the densities are not too high this rise can either be described by the DGLAP model [7] that assumes strong ordering in the transverse momentum k_T or by the BFKL model [8] that assumes strong ordering in x and random walk in k_T . Eventually at low enough x , the gluon-gluon fusion effects become important saturating the growth of the parton densities.

At the LHC the minimum accessible x in pp collisions decreases by a factor of about 10 for each 2 units of rapidity. This implies that a process with a hard scale of $Q \sim 10$ GeV and within the CASTOR/T2 detector acceptance can probe quark densities down $x \sim 10^{-6}$. Such processes include the production of forward jets and Drell-Yan electron pairs.

1. Forward Jets

A low- x parton distribution function (PDF) of the proton can be constrained by measuring single inclusive jet cross-section in HF. Figure 2 illustrates the $\log(x_{1,2})$ distribution for parton-parton scattering in pp collisions at

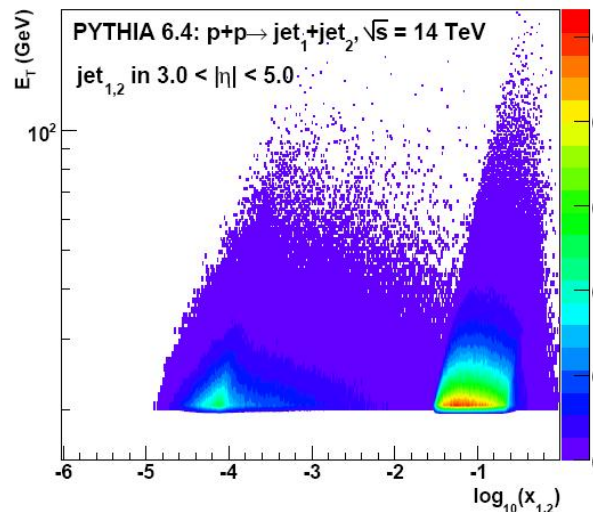


Figure 2: $\log(x_{1,2})$ distribution of two partons producing at least one jet with $E_T > 20$ GeV in the HF acceptance.

$\sqrt{s} = 14$ TeV requiring at least one jet with the transverse energy above 20 GeV in the HF acceptance. As can be seen, by measuring forward jets in HF one can probe x values as low as 10^{-5} . A detailed analysis of fully simulated and reconstructed QCD jet events generated with PYTHIA in the range $p_T = 20$ GeV/c–200 GeV/c in pp collisions at $\sqrt{s} = 14$ TeV for an integrated luminosity of 1 pb^{-1} shows that the momentum resolution for forward jets in HF is about 18% at $p_T = 20$ GeV/c and is gradually decreasing to 12% at $p_T \geq 100$ GeV/c [9].

A possibility to gain information on the full QCD evolution to study high order QCD reactions can be provided by measuring forward jets in the CASTOR calorimeter, that will allow to probe the parton densities down 10^{-6} . Apart from that, it has been found that a BFKL like simulation predicts more hard jets in the CASTOR acceptance than the DGLAP model. Therefore, measurements of forward jets in CASTOR can be used as a good tool to distinguish between DGLAP and non-DGLAP type of QCD evolution.

Further studies of low- x QCD can be made with Mueller-Navale dijet events, which are characterized by two jets with similar p_T but large rapidity separation. By measuring Mueller-Navale dijets in CASTOR and HF one can probe BFKL-like dynamics and small- x evolution.

2. Drell-Yan

Low- x proton PDFs can also be constructed by measuring electron pairs produced via the Drell-Yan process $qq \rightarrow \gamma^* \rightarrow e^+e^-$ within the acceptance of CASTOR and TOTEM-T2 station, whose usage is essential for detecting these events. Figure 3 illustrates the distribution of the invariant mass M of the ee system against the par-

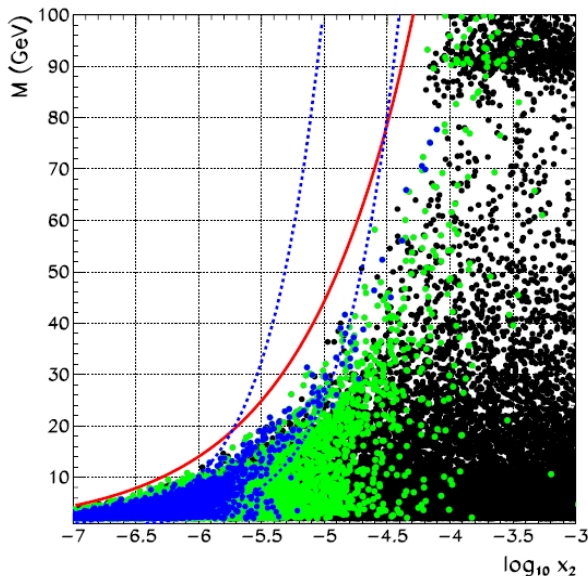


Figure 3: Acceptance of the CASTOR/T2 detectors for Drell-Yan electrons. See text for details.

ton momentum fraction x_2 of one of the quarks, where x_2 is chosen such that $x_1 \gg x_2$. In this figure, the solid line indicates the kinematic limit, whereas the region between the dotted lines is the acceptance window for both electrons to be detectable in CASTOR/T2. The green points show the events with at least one electron lying in CASTOR/T2 acceptance and the blue points indicate the events with both electrons present within the CASTOR/T2 acceptance, while the black points correspond to any of the Drell-Yan events generated with PYTHIA. As can be seen, by measuring two electrons in the CASTOR/T2 acceptance one can access x values down to 10^{-6} for $M > 10$ GeV [10]. Furthermore, measurements of Drell-Yan events in the CASTOR/T2 acceptance can be used to study QCD saturation effects. It has been found that the Drell-Yan production cross section is suppressed roughly by a factor of 2 when using a PDF with saturation effects compared to one without.

B. Diffraction

In pp collisions a diffractive process is a reaction $pp \rightarrow XY$, where X and Y can either be protons or low-mass systems which may be a resonance or a continuum state. In all cases, the final states X and Y acquire the energy approximately equal to that of the incoming protons and carry the quantum numbers of the proton as well as are separated by a Large Rapidity Gap (LRG). Diffraction in the presence of a hard scale can be described with perturbative QCD by the exchange of a colourless state of quarks or gluons, whereas soft diffraction at high energies is described in the Regge Theory [11] as a colourless exchange mediated by the Pomeron having the quan-

tum numbers of the vacuum. The cross section of hard diffractive processes can be factorized into generalized parton distributions and diffractive parton distributions functions (dPDF), which contain a valuable information about low- x partons. However, the factorization becomes broken when scattering between spectator partons takes place. This effect is quantified by the so-called rapidity gap survival probability that can be probed by measuring the ratio of diffractive to inclusive processes with the same hard scale. At the Tevatron, the ratio is found to be $O(1\%)$, whereas theoretical expectations at the LHC vary from a fraction of a percent to up to 30% [12].

The two main types of diffractive processes occurring in pp collisions are the single diffractive dissociation (SD) where one of the protons dissociates and the double diffractive dissociation (DD) where both protons are scattered into a low-mass system. The single-diffractive productions of W and dijets are in particular very interesting processes to study, since they are sensitive to the quark and gluon content of the PDFs, correspondingly. They both are hard diffractive processes that can provide information on the rapidity gap survival probability. A selection of such events can be performed using the multiplicity distributions of tracks in the central tracker and calorimeter towers in HF plus CASTOR exploiting the fact that diffractive events on average have lower multiplicity in the central region and in the "gap side" than non-diffractive ones. Feasibility studies to detect the SD productions of W [13] and dijets [14] have shown that the diffractive events peak in the regions of no activity in HF and CASTOR.

C. Exclusive dilepton production

Another interesting topic that is going to be studied at CMS is the exclusive dilepton production $pp \rightarrow pp\ell^+\ell^-$, which can either occur via Υ photoproduction $\gamma p \rightarrow \Upsilon \rightarrow \ell^+\ell^-$ or via the pure QED process $\gamma\gamma \rightarrow \ell^+\ell^-$ that has been observed by the CDF experiment at the Tevatron [15]. The latter is an elastic process whose production cross section is precisely known. As a result, it can potentially serve as an ideal calibration channel and is going to be used for measuring the luminosity at the LHC. Using this process an absolute luminosity calibration with the accuracy of 4% is feasible with 100 pb^{-1} of data [16]. The dominant background source for this mode is inelastic processes, where one of the proton in the process does not stay intact but dissociates. It can be significantly suppressed by applying a veto condition on activity in CASTOR and ZDC. Exclusive dilepton production occurring via Υ photoproduction is also a mode of interest, since the cross section of the Υ photoproduction process is sensitive to the generalized PDF for gluons in the proton. Finally, it should be noted that exclusive dimuon production is an ideal alignment channel for the proposed FP420 proton detectors.

D. Multi-parton interactions and forward energy flow

Multi-parton interactions (MPI) arise in the region of small- x where parton densities are large so that the likelihood of more than one parton interaction per event is high. According to all QCD models, the larger the collision energy the greater the contribution from multiple parton interactions to the hard scattering process. However, the dependence of the MPI cross section on the collision energy is not well known and needs to be studied. A good way to study multiple parton interactions is provided by the energy flow in the forward region, which is directly sensitive to the amount of parton radiation and MPI. Measurements of the forward energy flow will allow to discriminate between different MPI models, which vary quite a lot, and provide additional input to the determination of the parameters of the existing MPI models. Furthermore, measurements of forward particle production in pp and Pb-Pb collisions at LHC energies should help to significantly improve the existing constraints on ultra-high energy cosmic ray models. The primary energy and composition of the ultra-high energy cosmic rays are currently determined from Monte Carlo simulations using Regge-Gribov-based approaches [17] (where the primary particle production is dominated by forward and soft QCD interactions) with parameters constrained by the existing collider data at the $E_{lab} < 10^{15}$ eV, whereas the measured energies of the ultra-high energy cosmic rays extend up to 10^{20} eV and even beyond. At the LHC energy of $E_{lab} = 10^{17}$ eV, a more reliable determination of the cosmic ray energy and composition becomes possible. Finally, it should be emphasized that the forward energy flow has never previously been measured at a hadron collider.

IV. FIRST RESULTS FROM CMS

A. Observation of forward jets

A search for forward jets in the pseudorapidity range $3 < |\eta| < 5$ has been made as soon as the CMS detector has started to take collision data [18]. One of the first candidates of a forward dijet event recorded by CMS at $\sqrt{s} = 0.9$ TeV is shown in Figure 4. The displayed event includes one forward jet and one backward jet both with a corrected p_T above 10 GeV/c.

B. Measurement of the forward energy flow

Early measurements of the energy flow in the forward region of the CMS detector have been made with minimum bias events using the pp collision data sets collected at $\sqrt{s} = 0.9$ TeV and 2.36 TeV in the fall of 2009 and at $\sqrt{s} = 7$ TeV in March 2010 [19]. To select the events of interest the following conditions were imposed.

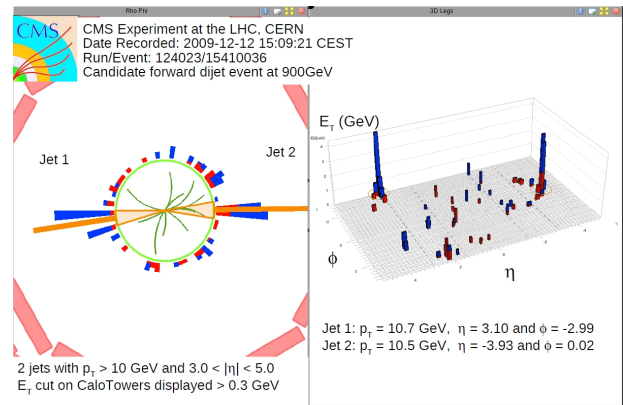


Figure 4: Display of an event with two forward jets.

First, the Beam Scintillator Counters (BSC) and the Beam Pick-up Timing for the eXperiments (BPTX), both are elements of the CMS detector monitoring system, were used to trigger the detector readout. The BSC devices are located at a distance of 10.86 m on both sides from the interaction point covering the pseudorapidity range $3.23 < |\eta| < 4.65$ and providing hit and coincidence signals with a time resolution of about 3 ns. Each BSC comprises 16 scintillator tiles. The two BPTX elements are located around the beam pipe at a distance of ± 175 m from the interaction point providing precise information on the bunch structure and timing of the incoming beam with a time resolution better than 0.2 ns. To select the minimum bias events with activity in the forward regions, the coincidence between a trigger signal in the BSC scintillators and BPTX signals was required for both beams.

Next, to ensure that the selected event is a collision candidate, the events were required to have at least one primary vertex reconstructed from at least 3 tracks with a z distance to the interaction point below 15 cm and a transverse distance from the z -axis smaller than 2 cm. Further cuts were applied to reject beam-scraping and beam-halo events. Finally, the energy threshold of 4 GeV has been imposed to suppress electronic noise in HF.

In this study, the measurement of energy flow has been made at detector level in the pseudorapidity range $3.15 < |\eta| < 4.9$ covered by the HF calorimeters. The energy flow ratio, estimated in this analysis, is defined as

$$R_{E_{flow}}^{\sqrt{s_1}\sqrt{s_2}} = \frac{\frac{1}{N_{\sqrt{s_1}}} \frac{dE_{\sqrt{s_1}}}{d\eta}}{\frac{1}{N_{\sqrt{s_2}}} \frac{dE_{\sqrt{s_2}}}{d\eta}}, \quad (1)$$

where $N_{\sqrt{s}}$ is the number of selected events, $dE_{\sqrt{s}}$ is the energy deposition integrated over ϕ in the region $d\eta$, $\sqrt{s_1}$ refers to either 2.36 TeV or 7 TeV, whereas $\sqrt{s_2}$ refers to 0.9 TeV. The pseudorapidity range is divided into five bins with a size of 0.35 in units of η following the transverse segmentation of the HF calorimeters. In Figures 5 and 6, the energy flow ratio is shown for different col-

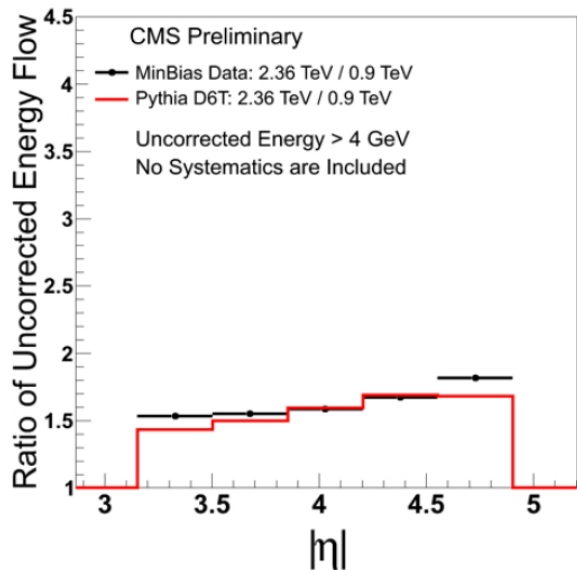


Figure 5: Energy flow ratio for $\sqrt{s_1} = 2.36$ TeV to $\sqrt{s_2} = 0.9$ TeV as a function of η . See text for details.

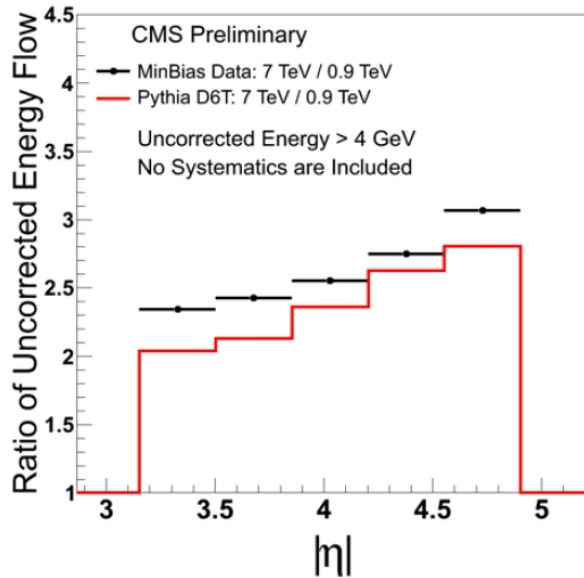


Figure 6: Energy flow ratio for $\sqrt{s_1} = 7$ TeV to $\sqrt{s_2} = 0.9$ TeV as a function of η . See text for details.

lision energies as the average of the HF(+) and HF(-) responses. In these plots, uncorrected data without systematic uncertainties are compared to simulated events obtained from PYTHIA tune D6T. As can be clearly seen, the energy flow gets larger at forward rapidities and with increasing centre-of-mass energy. Apart from that, it should be noted that the obtained results do approximately agree with the Monte Carlo predictions. However, no conclusions on the quality of the description can be drawn in this early study due to the missing systematic effects.

V. CONCLUSIONS

A very rich forward physics program can be made with the CMS detector at the LHC due to the unprecedented kinematic coverage of the forward region. All the CMS forward detectors have been successfully commissioned in 2009 and currently take collision data. The first measurement of the forward energy flow has been performed and forward jets at $|\eta| > 3$ have been observed for the first time at hadron colliders.

VI. ACKNOWLEDGMENTS

I am very grateful to Hannes Jung, Kerstin Borrás and many other colleagues working in the CMS forward physics community for fruitful discussions and kind suggestions.

-
- [1] *CMS Collaboration*. The CMS Experiment at the CERN LHC, 2008 JINST 3 S8004.
 - [2] *A. Penzo et al.* The CMS-HF quartz fiber calorimeters, 2009 J. Phys.: Conf. Ser. 160 012014.
 - [3] *E. Norbeck et al.* Physics at Very Small Angles with CASTOR at CMS, CERN-CMS-CR-2006-028.
 - [4] *O. Grachov et al.* Status of Zero Degree Calorimeter for CMS Experiment, arXiv:nucl-ex/0608052v2.
 - [5] *TOTEM Collaboration*. The TOTEM Experiment at the CERN Large Hadron Collider, 2008 JINST 3 S08007.
 - [6] *J. Pater*. The FP420 Project: The challenge of measuring forward protons at the LHC, 2008 J. Phys.: Conf. Ser. 110 092022
 - [7] *V.N. Gribov and L.N. Lipatov*. Sov. J. Nucl. Phys. 15 (1972), 438.
 - [8] *I.I. Balitskii and L. N. Lipatov*. Sov. J. Nucl. Phys. 28

- (1978) 822.
- [9] *S. Cerci and D. d'Enterria*. Low-x QCD studies with forward jets in proton-proton collisions at 14 TeV, AIP Conf.Proc.1105:28-32, 2009
- [10] *CMS and TOTEM Collaborations*. CERN/LHCC 2006-039/G-124 (2006).
- [11] *P. Collins*. An Introduction to regge Theory and High-Energy Physics, Cambridge University Press, 1977.
- [12] *B. Cox et al*. Phys.Comm. 144 (2002) 104; *V. Khoze et al*. arXiv:0802.0177 [hep-ph]
- [13] *CMS Collaboration*. Study of single-diffractive production of W bosons at the LHC, CERN CMS-PAS-DIF-07-002 (2007).
- [14] *CMS Collaboration*. Observation of Single-Diffractive Production of Di-jets at the LHC, CERN CMS-PAS-FWD-08-002 (2008).
- [15] *CDF Collaboration*. Observation of Exclusive Electron-Positron Production in Hadron-Hadron Collisions, Phys. Rev.Lett. 98 (2007) 112001.
- [16] *CMS Collaboration*. Exclusive Dilepton Production, CERN CMS-PAS-FWD-07-001 (2007).
- [17] *V. Gribov*. Sov. Phys. JETP 26 414 (1968).
- [18] *CMS Collaboration*. Event displays of forward jets at 900 GeV, CERN-CMS-DP-2010-006 (2010).
- [19] *CMS Collaboration*. Energy Flow Ratios in HF at Different Collision Energies, CERN-CMS-DP-2010-007 (2010).